Optical Pumping With Laser-Induced Fluorescence

15 June 1996

Prepared by

J. C. CAMPARO and S. B. DELCAMP
Electronics Technology Center
Technology Operations

Prepared for

SPACE AND MISSILE SYSTEMS CENTER
AIR FORCE MATERIEL COMMAND
2430 E. El Segundo Boulevard
Los Angeles Air Force Base, CA 90245

19961017 065

Engineering and Technology Group

THE AEROSPACE
CORPORATION
El Segundo, California

This report was submitted by The Aerospace Corporation, El Segundo, CA 90245-4691, under Contract No. F04701-93-C-0094 with the Space and Missile Systems Center, 2430 E. El Segundo Blvd., Los Angeles Air Force Base, CA 90245. It was reviewed and approved for The Aerospace Corporation by T. A. Galantowicz Principal Director, Electronics Technology Center. Col. C. Whited was the project officer for the Mission-Oriented Investigation and Experimentation (MOIE) program.

This report has been reviewed by the Public Affairs Office (PAS) and is releasable to the National Technical Information Service (NTIS). At NTIS, it will be available to the general public, including foreign nationals.

This technical report has been reviewed and is approved for publication. Publication of this report does not constitute Air Force approval of the report's findings or conclusions. It is published only for the exchange and stimulation of ideas.

C. WHITED, Col. USAF
SMC/SD

REPORT DOCUMENTATION PAGE

Form Approved
OMB No. 0704-0188

1. AGENCY USE ONLY (*Leave blank*)	2. REPORT DATE 15 June 1995	3. REPORT TYPE AND DATES COVERED

4. TITLE AND SUBTITLE

Optical Pumping with Laser-Induced Fluorescence

5. FUNDING NUMBERS

F04701-93-C-0094

6. AUTHOR(S)

J. C. Camparo and S. B. Delcamp

7. PERFORMING ORGANIZATION NAME(S) AND ADDRESS(ES)

The Aerospace Corporation
Technology Operations
El Segundo, CA 90245-4691

8. PERFORMING ORGANIZATION REPORT NUMBER

TR-95(5925)-8

9. SPONSORING/MONITORING AGENCY NAME(S) AND ADDRESS(ES)

Space and Missile Systems Center
Air Force Materiel Command
2430 E. El Segundo Boulevard
Los Angeles Air Force Base, CA 90245

10. SPONSORING/MONITORING AGENCY REPORT NUMBER

SMC-TR-96-16

11. SUPPLEMENTARY NOTES

12a. DISTRIBUTION/AVAILABILITY STATEMENT

Approved for public release; distribution unlimited

12b. DISTRIBUTION CODE

13. ABSTRACT (*Maximum 200 words*)

We describe a new procedure for optical pumping that is based on laser-induced fluorescence (LIF). The procedure is demonstrated by optically exciting a sample of Rb^{85} atoms, which then create a population imbalance between the ground state hyperfine levels of Rb^{87} by "LIF depopulation pumping." Though optical pumping with this technique increases the intensity-dependent light-shift coefficient (i.e., ac Stark shift) of the Rb^{87} 0–0 hyperfine transition, it reduces the frequency-dependent light-shift coefficient by at least an order of magnitude. Since the stabilization of the diode laser wavelength is a significant challenge in the development of laser-pumped gas-cell atomic clocks, it is anticipated that optical pumping with LIF will be of benefit to atomic clock technology.

14. SUBJECT TERMS

Optical pumping, Laser-induced fluorescence

15. NUMBER OF PAGES
10

16. PRICE CODE

17. SECURITY CLASSIFICATION OF REPORT	18. SECURITY CLASSIFICATION OF THIS PAGE	19. SECURITY CLASSIFICATION OF ABSTRACT	20. LIMITATION OF ABSTRACT
UNCLASSIFIED	UNCLASSIFIED	UNCLASSIFIED	

Preface

Contents

Figures

Table

1. Introduction

In the early eighties, Volk et al. [1] discovered that a rubidium (Rb) atomic clock, which is based on the 0–0 ground state hyperfine transition in Rb^{87} (i.e., the $[F_g = 2, m_F = 0] - [F_g = 1, m_F = 0]$ transition) [2], could be operated by tuning a diode laser to a Rb^{85} optical transition in an isotopically mixed Rb vapor. This observation was surprising, because it implied that optical excitation of one Rb isotope created a population imbalance between the ground state hyperfine levels of the other Rb isotope. Since the optical transitions of the two isotopes were well resolved, implying that the laser could not have been optically pumping the Rb^{87} population directly, the authors suggested a collisional mechanism for the creation of Rb^{87} ground state hyperfine polarization (i.e., $\langle I \cdot S \rangle_{87} \neq 0$, where I is the nuclear spin and S is the electronic spin). They hypothesized that laser optical pumping of Rb^{85} created $\langle I \cdot S \rangle_{85} \neq 0$, and that Rb^{85}–Rb^{87} spin-exchange collisions then transferred this hyperfine polarization to the Rb^{87} population.

Unfortunately, there are several problems with this mechanism. First, in the absence of Rb^{85} electron spin polarization, spin-exchange will simply act as an electron-randomization mechanism [3]. Thus, Volk et al.'s hypothesis requires $\langle S_z \rangle_{85} \neq 0$, and how this spin polarization could have been achieved is a problematic feature of the hypothesis. A non-zero electronic spin polarization in the Rb^{85} ensemble could have been created if their laser has some degree of elliptical polarization. However, diode lasers typically display a high degree of linear polarization [4], though more complicated states of optical polarization in these devices have been observed [5]. Alternatively, elliptically polarized light might have been created within the vapor itself via the nonlinear Faraday effect [6]; or a non-zero Rb^{85} electronic spin polarization might have been created by some more complicated spin-exchange process, for example the spontaneous spin polarization process of Forston and Heckel [7]. However, even if $\langle S_z \rangle_{85} \neq 0$, it might not be possible for spin-exchange to give rise to a significant 0–0 hyperfine population imbalance in the Rb^{87} ensemble. If it is assumed that spin-exchange is rapid enough so as to set up a spin-temperature equilibrium in the Rb^{87} population, then the density matrix operator describing the population distribution among the ground state sublevels can be written as [8]

$$\rho = C \exp(\beta F_z) , \tag{1}$$

where β is the spin-temperature parameter, F_z is the azimuthal projection of the total atomic angular momentum ($F = I + S$ for the alkali ground state), and C is a normalization factor:

$$C = \frac{\sinh(\beta/2)}{\sinh[\beta(I+1)] + \sinh(\beta I)} . \tag{2}$$

Under such conditions, Eq. (1) predicts that $\rho_{87}(F = 2, m_F = 0) = C = \rho_{87}(F = 1, m_F = 0)$, so that there could be no 0–0 hyperfine signal for the atomic clock operation.

A more plausible mechanism, first suggested by Happer [9], is based on laser-induced fluorescence (LIF). Fig. 1 is a partial energy level diagram of Rb^{85} and Rb^{87} showing that D_2 transitions ($5^2P_{3/2}$–$5^2S_{1/2}$ at 780.2 nm) corresponding to the $F_g = 3$ ground state hyperfine level of Rb^{85} are nearly resonant with D_2 transitions corresponding to the $F_g = 2$ hyperfine level of Rb^{87} for a room temperature vapor. Furthermore, it is to be noted that radiation trapping in the alkali vapors is significant even at relatively low vapor densities [10], and that under conditions of radiation trapping fluorescent photons diffuse to the line wings [1]. Thus, D_2 Rb^{85} laser-induced fluorescence, specifically the $F_g = 3$ component of the fluorescence, will be reabsorbed by Rb^{87} atoms in the $F_g = 2$ hyperfine level. As a consequence of this "LIF depopulation pumping" of Rb^{87}, a Rb^{87} hyperfine polarization will be created.
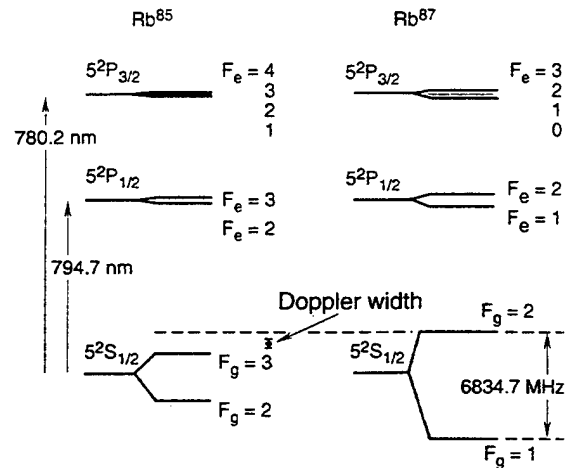

Fig. 1. Partial energy level diagram for Rb^{85} and Rb^{87}. Within each fine structure level, the hyperfine energy level spacings are drawn to scale.

---

[1] For examples of how radiation trapping at a moderate temperature can cause distortions of alkali fluorescent spectra, see Ref. [11].

It is to be noted that three hallmarks of this LIF mechanism are: (1) that it can occur with linearly polarized light, (2) that it is *resonant* with Rb^{85} excitation, and (3) that the optical pumping process results in a Rb^{87} population transfer from the $F_g = 2$ hyperfine level to the $F_g = 1$ hyperfine level.

In the following section of this paper we describe an experiment examining the creation of Rb^{87} hyperfine polarization due to Rb^{85} optical excitation, and show that the mechanism of LIF depopulation pumping is consistent with observation. This is then followed by a section dealing with the light shifts (i.e., ac Stark shifts) associated with this optical pumping process. As will be shown, for the same hyperfine transition signal amplitudes, the frequency dependent light-shift coefficient associated with LIF depopulation pumping is at least an order of magnitude smaller than that associated with standard depopulation pumping. Conversely, the (relative) intensity dependent light-shift coefficient associated with LIF depopulation pumping is larger than that associated with standard depopulation pumping. Since the predicted performance capability of a diode-laser-pumped gas-cell atomic clock is strongly influenced by laser frequency fluctuations [12], an atomic clock based on LIF depopulation pumping could have considerable practical value.

2. Experiment

Fig. 2 shows our basic experimental arrangement. A cylindrical resonance cell ($L = 3$ cm and $R = 1.25$ cm), containing natural Rb (72% Rb^{85} and 28% Rb^{87}) along with 14 Torr of neon, was located in the path of two crossed diode laser beams; the cylindrical axis of the resonance cell was parallel to the probe beam's propagation direction. The resonance cell was located in a 0.19 G magnetic field in order to isolate the 0–0 hyperfine transition, and the pool of liquid alkali metal in the resonance cell was maintained at about 63°C, implying an alkali vapor density of $\sim 7 \times 10^{11}$ cm^{-3} [13]. The neon was present as a buffer gas to impede Rb diffusion to the resonance cell walls which are highly depolarizing.

The probe laser at 794.7 nm had a linewidth of 56 MHz, and an intensity of 1.1 μW/cm^2 after attenuation by an optical density filter. The probe beam filled the resonance cell's cross-sectional area, and it was always tuned to the $5^2P_{1/2}(F_e = 2)$–$5^2S_{1/2}(F_g = 1)$ transition of Rb^{87}. Thus, its transmission through the vapor essentially monitored the Rb^{87} population in the $F_g = 1$
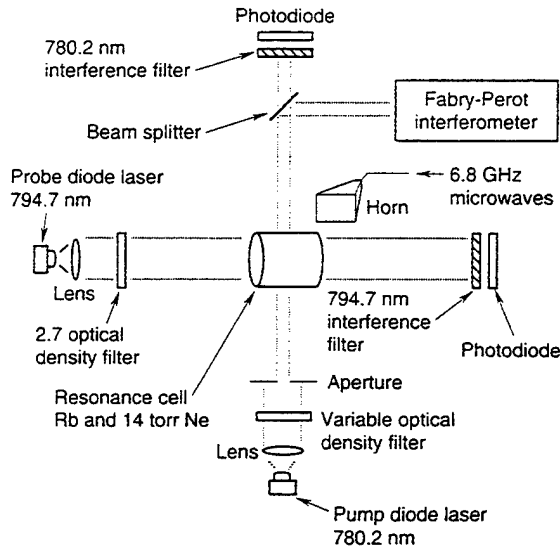

Fig. 2. Experimental arrangement as described in the text.

hyperfine level. For reference purposes, Fig. 3 shows the absorption profile of the probe beam, along with an indication of the ground state hyperfine levels involved in the transitions. (Due to the large $5^2P_{1/2}$ excited state hyperfine splitting in Rb^{87}, the two outer profiles appear as doublets.) Note that the pressure and Doppler broadening of the optical transitions were not too severe, so that the transitions of the two isotopes were well resolved. The pump laser at 780.2 nm had a linewidth of 40 MHz, and an intensity of 7.6 mW/cm^2. An aperture placed in the pump beam path reduced the beam diameter to 0.8 cm, so that the probe beam would completely overlap the pump beam volume. After passing through the alkali vapor, the pump beam was split in two. One portion of the pump beam was detected with a photodiode, and the transmitted light intensity monitored by this photodiode was used to tune the pump
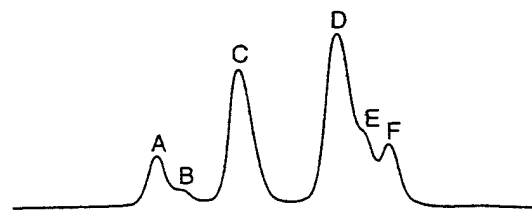
Fig. 3. Probe laser's absorption spectrum for D_1 excitation (i.e., $5^2P_{1/2}$–$5^2S_{1/2}$): (A) Rb^{87} ($F_e = 2$)–($F_g = 1$); (B) Rb^{87} ($F_e = 1$)–($F_g = 1$); (C) Rb^{85} ($F_e = 2, 3$)–($F_g = 2$); (D) Rb^{85} ($F_e = 2, 3$)–($F_g = 3$); (E) Rb^{87} ($F_e = 2$)–($F_g = 2$); (F) Rb^{87} ($F_e = 1$)–($F_g = 2$). Note that the excited state hyperfine splitting in Rb^{87} is resolved.

2

beam to an atomic resonance. The other portion of the pump beam passed into a confocal Fabry–Pérot interferometer having a free-spectral-range of 2 GHz and a finesse of about 150. The signal from the interferometer was observed on a calibrated oscilloscope, and was used to measure detunings of the pump beam from an atomic resonance. The degree of linear polarization of the pump beam was measured, and found to be 99.9%.

The output of a frequency synthesizer was centered at 13.349 MHz, and slowly ramped through approximately ± 20 MHz about that value. This output was then multiplied up to 6834.7 MHz, which corresponds to the ground state hyperfine splitting in Rb^{87}; the microwave signal strength was large enough to saturate the 0–0 hyperfine transitions. In the absence of resonance microwaves, a population pumping process (e.g., optical pumping) will cause a change in the Rb^{87} $F_g = 1$ hyperfine level population, and consequently a change in the magnitude of probe laser light transmitted by the resonance cell. As the microwaves were tuned across the ground state Rb^{87} 0–0 hyperfine transition, the population imbalance between the two Rb^{87} ground state hyperfine levels was reduced, with a concomitant change in the magnitude of transmitted probe laser light. The probe laser's transmission thus acted to trace out the Rb^{87} 0–0 ground state hyperfine transition lineshape. The important point to note for the present purposes, however, is that when the hyperfine resonance corresponded to an *increase* in probe laser light absorption, it could be inferred that the operative population pumping process had *reduced* the atomic population in the Rb^{87} $F_g = 1$ hyperfine level. Conversely, when the hyperfine resonance corresponded to a decrease in probe laser light absorption, the population pumping process must have increased the atomic population in the Rb^{87} $F_g = 1$ hyperfine level.

3. Results

Fig. 4 illustrates the Rb^{87} 0–0 ground state hyperfine transition obtained in the present experiment under different optical excitation conditions. In the figure, probe laser absorption is shown as a function of time or, what is equivalent, microwave frequency. For Fig. 4a the pump beam was blocked, so that the small resonant increase in probe absorption was due solely to residual probe optical pumping. Note that since optical pumping by the probe necessarily reduced the number of atoms in the absorbing state, the figure shows the 0–0 hyper-

fine transition as an increase in probe absorption. Fig. 4b resulted when the pump beam was unblocked and tuned to the $F_g = 1$ D_2 transition of Rb^{87}. The 0–0 hyperfine transition again appeared as an increase in probe absorption (albeit a larger increase), since the pump now acted more efficiently to reduce the number of atoms in the probe absorbing state. Tuning the pump beam to the $F_g = 2$ D_2 transition of Rb^{87} resulted in an optical pumping process that increased the number of atoms in the $F_g = 1$ state, and, as Fig. 4c shows, the 0–0 hyperfine transition corresponded to a decrease in probe absorption. Finally, when the pump was tuned to the $F_g = 2$ D_2 transition of Rb^{85}, Fig. 4d resulted. Since the 0–0 hyperfine transition appears as a decrease in probe absorption, the process creating the Rb^{87} population imbalance must have been increasing the population density in the Rb^{87} $F_g = 1$ hyperfine level.

Several other characteristics regarding the 0–0 hyperfine transition lineshape are worth noting. First, the resonance signal of Fig. 4d could be observed with an optical density of 1.0 in the pump beam path, and a similar (decreasing absorption resonance) was observed when the pump laser was tuned to the $F_g = 3$ D_2 transition of Rb^{85}. Additionally, the amplitude of the 0–0 hyperfine transition lineshape showed a clear resonant behavior as the pump laser was tuned about the $F_g = 2$ D_2 transition of Rb^{85}; this is illustrated in Fig. 5. Given these results, the LIF depopulation pumping mechanism described above seems the most likely explanation for the Rb^{87} population imbalance generated by Rb^{85} optical excitation.

4. Light shifts

In addition to optical pumping, a laser also gives rise to light shifts of the 0–0 hyperfine transition $\Delta \nu_{LS}$. These shifts arise from a second order interaction between the laser electric field, E, and the atom's induced dipole moment, P: $h\Delta \nu_{LS} = -P \cdot E/2 = -\alpha(\omega) \Phi/2$, where $\alpha(\omega)$ is the frequency dependent ground state polarizability of the atom and Φ is the laser intensity [14]. Happer and Mathur [15,16] have performed detailed studies of the light shift in alkali atoms, and find that for standard hyperfine depopulation pumping [2] the laser frequency dependence of the light shift should be quite strong (i.e., $\partial(\Delta \nu_{LS})/\partial\omega_L$

---

[2] By standard depopulation pumping, we mean an optical pumping process like that giving rise to the hyperfine transition of Fig. 4a.

3

(A)   (B)
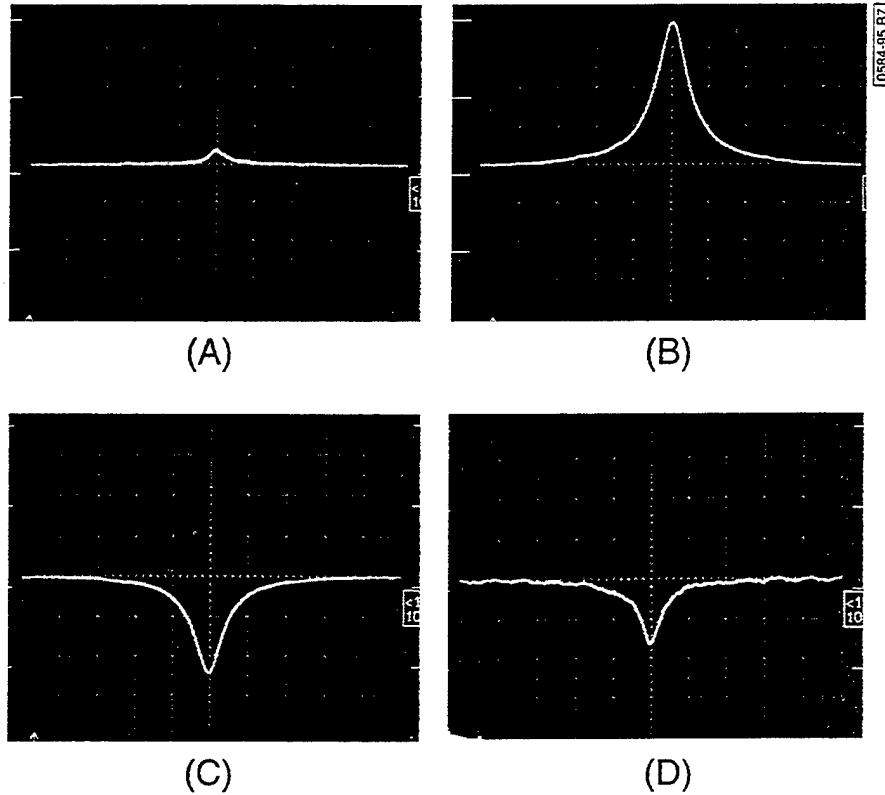
(C)   (D)

Fig. 4. Oscilloscope traces of the Rb^{87} 0–0 hyperfine transition lineshapes under varied optical excitation conditions with the probe laser tuned to the Rb^{87} $D_1|5^2P_{1/2}$ $(F_e=2)-5^2S_{1/2}(F_g=1)\}$ transition. The photocurrent generated by the probe laser's photodiode was detected across 200 kΩ, and amplified by 200 before being displayed on the oscilloscope: (a) pump laser blocked, 20 mV/cm; (b) pump laser exciting Rb^{87} atoms out of $F_g=1$ hyperfine level, 20 mV/cm; (c) pump laser exciting Rb^{87} atoms out of $F_g=2$ hyperfine level, 20 mV/cm; (d) pump laser exciting Rb^{85} atoms out of the $F_g=2$ hyperfine level, 10 mV/cm.
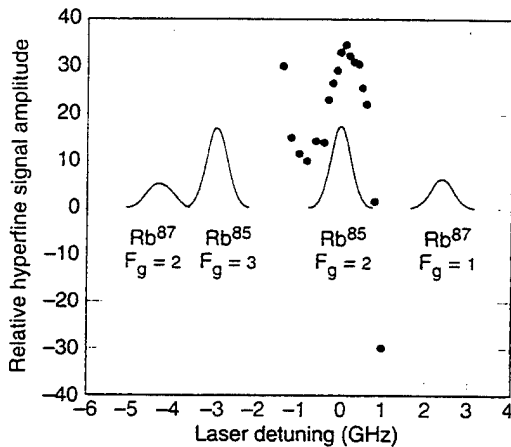

Fig. 5. Resonant nature of the Rb^{87} hyperfine transition signal with laser tuning about the $F_g=2$ Rb^{85} optical transition. The closed circles correspond to our measurements of the hyperfine resonance amplitude. Contrary to Fig. 4 a positive amplitude corresponds to decreasing absorption, while a negative amplitude corresponds to increasing absorption. The solid curves are simply meant as markers to show the Doppler broadened absorption profiles, and include the influence of the $5^2P_{1/2}$ excited state hyperfine structure.

relatively large, where ω_L is the laser frequency), while the laser intensity dependence should be zero (i.e., $\partial(\Delta\nu_{LS})/\partial\Phi=0$). These expectations have been borne out numerous times in the past [1,17–20]. However, for our LIF depopulation pumping experiment, the laser is far-detuned from a Rb^{87} optical transition, and consequently theory predicts just the opposite situation: $\partial(\Delta\nu_{LS})/\partial\omega_L\cong 0$ and $\partial(\Delta\nu_{LS})/\partial\Phi$ non-zero.

To test these expectations, we first measured the frequency and intensity dependence of the light shift for standard depopulation pumping. The frequency dependence was established by tuning the pump laser to the $F_g=1$ D_2 transition of Rb^{87}, and inserting a 2.6 optical density filter in the pump beam path so that the magnitude of the hyperfine resonance was equivalent to that shown in Fig. 4d (i.e., the same as for LIF depopulation pumping). The change in center position of the hyperfine resonance was then recorded for the pump laser detuned by $+400$ and -400 MHz from resonance, and the experiment was repeated several times to obtain an estimate of the measurement uncer-

tainty. The intensity dependence was established by keeping the pump laser tuned to the $F_g = 1$ D_2 transition of Rb^{87}, and examining the change in the hyperfine resonance's center position as the optical density filter in the pump beam path was changed from 2 to 3. Again, the experiment was repeated several times to obtain an estimate of the measurement uncertainty. A similar set of measurements was performed for LIF depopulation pumping with the pump laser tuned to the $F_g = 2$ D_2 transition of Rb^{85}, except that for the intensity dependence measurements the change in the optical density filter was from 0 to 1.

The results of these measurements are collected in Table 1, where for later reference the values are given in terms of fractional-frequency (i.e., $\Delta\nu_{LS}/\nu_{hfs}$). Though we quote an intensity dependent light-shift coefficient in terms of fractional-frequency/ $\mu W \cdot cm^{-2}$, for comparative purposes it is better to consider the intensity dependent light-shift coefficient quoted in terms of percentile light intensity change, since the absolute light intensity required for the two optical pumping processes differs appreciably. As the results demonstrate, the frequency dependent light-shift coefficient of the 0–0 hyperfine transition is at least an order of magnitude smaller than that obtained in standard depopulation pumping, while the relative intensity dependent light-shift coefficient is larger.

5. Discussion

As demonstrated in the previous section, LIF depopulation pumping trades an enhanced sensitivity to (relative) laser intensity fluctuations for a diminished sensitivity to laser frequency fluctuations, and it is just this decreased sensitivity to laser frequency noise that provides LIF depopulation pumping with its principal advantage over standard depopulation pumping. As an example, consider diode laser optical pumping in the gas-cell atomic frequency standard (i.e., atomic clock), which has been lauded as a means of achieving

"maser-like" performance in the compact device. Essentially, the use of diode lasers allows for very efficient standard depopulation pumping, resulting in large signal-to-noise ratios and narrow hyperfine transition lineshapes. Theory predicts that by averaging the atomic standard's output frequency for several minutes it should be possible to achieve a shot-noise limited fractional-frequency stability better than 10^{-15} [12]. In order to achieve this expectation though, it is necessary to tightly stabilize the laser frequency, since laser frequency instability maps onto the atomic frequency standard's output as a consequence of the light-shift effect. Measurements of the light-shift coefficient in laser-pumped gas-cell clock's have been found to be $\sim 2 \times 10^{-11}$/MHz [21], implying that the theoretical expectation necessitates locking the diode laser to within 50 Hz of an atomic resonance for periods of minutes.

In the course of our experiment, we measured the hyperfine signal's amplitude and linewidth for LIF depopulation pumping. On the basis of those measurements, we estimated that the resulting signal could have given rise to a shot-noise limited performance of $3 \times 10^{-11}/\sqrt{\tau}$, where τ is the frequency-averaging time [22]. This was obtained without any optimization of resonance cell temperature or beam geometry, and one would anticipate that the value could be considerably improved by increasing the cross-sectional area of the probe beam and the resonance cell. The significance of the result, however, is that it indicates that LIF depopulation has a capability to achieve reasonable signal-to-noise levels. Moreover, since LIF depopulation pumping has a reduced frequency dependent light-shift coefficient, the laser frequency locking requirements for such an atomic clock would be considerably relaxed compared to an atomic clock based on standard depopulation pumping.

Of course, if LIF depopulation pumping was to be employed in an atomic clock, the fluctuations in laser intensity would need to be restricted. However, this may not be too serious a technological challenge.

Table 1
Results of experiment comparing light shifts in standard and LIF depopulation pumping

	Unit	Standard depopulation pumping	LIF depopulation pumping
$\partial(\Delta\nu_{LS})/\partial\omega_L$	MHz^{-1}	$(-1.9\pm0.3)\times10^{-11}$	$(0.08\pm0.27)\times10^{-11}$
$\partial(\Delta\nu_{LS})/\partial\Phi$	$\mu W^{-1}\cdot cm^2$	$(-3\pm4)\times10^{-11}$	$(-2.5\pm0.1)\times10^{-12}$
	%$^{-1}$	$(-1.2\pm1.7)\times10^{-11}$	$(-1.09\pm0.06)\times10^{-10}$

5

Tsuchida and Tako [23] have found that the intensity noise for a frequency stabilized laser, operating without any control on laser intensity, has a flicker-noise Allan standard deviation [3], $\sigma_{\Delta P/P}(\tau)$, of 3×10^{-5}. Consequently, employing the intensity dependent light-shift coefficient obtained in the present work, their result would imply a flicker-noise light-shift contribution to the clock performance of 3×10^{-13}. Moreover, by employing an external electro–optic modulator it might be possible to reduce this level of intensity noise still further [26]. Thus, LIF depopulation pumping could be advantageous for situations where light shifts are problematic; specifically, diode laser optical pumping in gas-cell atomic clocks.

References

[1] C.H. Volk, J.C. Camparo and R.P. Frueholz, in: Proc. 13th Annual Precise Time and Time Interval (PTTI) Applications and Planning Meeting (US Naval Observatory, Washington, DC, 1981) pp. 631–640.

[2] J. Vanier and C. Audoin, The quantum physics of atomic frequency standards, Vol. 2 (Adam Hilger, Bristol, 1989).

[3] W. Happer, Rev. Mod. Phys. 44 (1972) 169.

[4] J.C. Camparo, Contemp. Phys. 26 (1985) 443.

[5] T.L. Paoli, IEEE J. Quantum Electron. QE-11 (1975) 489.

[6] S.I. Kanorsky. A. Weis, J. Wurster and T.W. Hansch, Phys. Rev. 47 (1993) 1220.

[7] N. Fortson and B. Heckel, Phys. Rev. Lett. 59 (1987) 1281.

[8] L.W. Anderson and A.T. Ramsey, Phys. Rev. 132 (1963) 712; W. Happer and A.C. Tam, Phys. Rev. A 16 (1977) 1877.

[9] W. Happer, private communication.

[10] B.P. Kibble, G. Copley and L. Krause, Phys. Rev. 153 (1967) 9.

[11] T. Tako, Y. Koga and I. Hirano, Jpn. J. Appl. Phys. 14 (1975) 591; F. Vermeersch, V. Fiermans, J. Ongena, H.A. Post and W. Wieme, J. Phys. B 21 (1988) 1933.

[12] J.C. Camparo and R.P. Frueholz, J. Appl. Phys. 59 (1986) 3313.

[13] T.J. Killian, Phys. Rev. 27 (1926) 578.

[14] S. Pancharatnam, J. Opt. Soc. Am. 56 (1966) 1636.

[15] W. Happer and B.S. Mathur, Phys. Rev. 163 (1967) 12.

[16] B.S. Mathur, H. Tang and W. Happer, Phys. Rev. 171 (1968) 11.

[17] M. Arditi and J-L. Picque, J. Phys. B 8 (1975) L331.

[18] J.C. Camparo, R.P. Frueholz and C.H. Volk, Phys. Rev. A 27 (1983) 1914.

[19] M. Hashimoto and M. Ohtsu, IEEE J. Quantum Electron. QE-23 (1987) 446.

[20] A. Michaud, P. Tremblay and M. Tetu, IEEE Trans. Instrum. Meas. 40 (1991) 170.

[21] M. Hashimoto and M. Ohtsu, IEEE J. Quantum Electron. QE-23 (1987) 446; L.A. Budkin, V.L. Velichanskii, A.S. Zibrov, A.A. Lyalyaskin, M.N. Penenkov and A.I. Pikhtelev, Sov. J. Quantum Electron. 20 (1990) 301.

[22] J. Vanier and L-G. Bernier, IEEE Trans. Instrum. Meas. IM-30 (1981) 277.

[23] H. Tsuchida and T. Tako, Jpn. J. Appl. Phys. 22 (1983) 1152.

[24] S.R. Stein, Frequency and time – their measurement and characterization, in: Precision frequency control, Vol. 2, eds. E.A. Gerber and A. Ballato (Academic Press, New York, 1985) Ch. 12.

[25] S. Yamaguchi and M. Suzuki, IEEE J. Quantum Electron. QE-19 (1983) 1514.

[26] V.N. Korolev, A.V. Marugin, A.V. Kharachev and V.B. Tsaregradskii, Sov. Phys. Tech. Phys. 34 (1989) 863.

---

[3] Fig. 3 of Ref. [23] shows an Allan standard deviation for the intensity noise that increases linearly with averaging time beyond one second. This is the hallmark of a deterministic drift; see Ref. [24]. The power drift of the laser, however, can be significantly reduced if not eliminated; see Ref. [25].